blood

2005 105: 1970-1976
Prepublished online Oct 26, 2004;
doi:10.1182/blood-2004-04-1469

Inhibition of vascular endothelial growth factor receptor 2–mediated endothelial cell activation by Axl tyrosine kinase receptor

Margherita Gallicchio, Stefania Mitola, Donatella Valdembri, Roberto Fantozzi, Brian Varnum, Gian Carlo Avanzi and Federico Bussolino

Blood (print ISSN 0006-4971, online ISSN 1528-0020), is published semimonthly by the American Society of Hematology, 1900 M St, NW, Suite 200, Washington DC 20036.

Inhibition of vascular endothelial growth factor receptor 2–mediated endothelial cell activation by Axl tyrosine kinase receptor

Margherita Gallicchio, Stefania Mitola, Donatella Valdembri, Roberto Fantozzi, Brian Varnum, Gian Carlo Avanzi, and Federico Bussolino

GAS6, the product of a growth arrest specific *(GAS)* gene, is the ligand of the tyrosine kinase receptor Axl. GAS6 and Axl are both expressed in endothelial cells, where they are involved in many processes such as leukocyte transmigration through capillaries and neointima formation in injured vessels. Here, we show that Axl stimulation by GAS6 results in inhibition of the ligand-dependent activation of vascular endothelial growth factor (VEGF) receptor 2 and the consequent activation of an angiogenic program in vascular endothelial cells. GAS6 inhibits chemotaxis of endothelial cells stimulated by VEGF-A isoforms, but not that triggered by fibroblast growth factor-2 or hepatocyte growth factor. Furthermore, it inhibits endothelial cell morphogenesis on Matrigel and VEGF-A–dependent vascularization of chick chorion allantoid membrane. GAS6 activates the tyrosine phosphatase SHP-2 (SH2 domain-containing tyrosine phosphatase 2), which is instrumental in the negative feedback exerted by Axl on VEGF-A activities. A dominant-negative SHP-2 mutant, in which Cys 459 is substituted by Ser, reverted the effect of GAS6 on stimulation of VEGF receptor 2 and endothelial chemotaxis triggered by VEGF-A. These studies provide the first demonstration of a cross talk between Axl and VEGF receptor 2 and add new information on the regulation of VEGF-A activities during tissue vascularization. (Blood. 2005;105:1970-1976)

Introduction

Axl is a 140-kDa protein which belongs to a subfamily of tyrosine kinase receptor (RTK) that includes also Mer and Rse. These receptors are characterized by the presence of 2 immunoglobulin-like domains and 2 fibronectin–type III domains in the extracellular region and a distinctive intracellular kinase domain.[1-3] Axl was first isolated from the DNA of patients with chronic myelogenous leukemia, but subsequently its expression was demonstrated in mammalian cells of vascular, immune, and reproductive systems.[1,4-6] Axl is involved in cell-cell aggregation,[7] in the maintenance of a wide variety of cell types in adult tissues,[6] and in homeostatic regulation of immune system.[8]

GAS6, a protein codified by a growth arrest specific gene, is a member of the vitamin K–dependent protein family. GAS6 has 42% amino acid identity to protein S, a serum protein that negatively regulates blood coagulation. GAS6 is composed of characteristic structural motifs: a γ-carboxylated amino-terminus domain followed by 4 epidermal growth factor–like domains and by a set of tandem G domains similar to those of sex hormone binding globulin.[9] GAS6 binds with different affinities and activates the kinase activity of each Axl family member.[10-12] GAS6 shows the higher affinity for Axl, and its interaction generally triggers antiapoptotic signals, resulting in an augmented cell survival. In some cell types it regulates homotypic and heterotypic adhesion,[4,13] promotes proliferation,[5,14] survival,[15-18] and motility[19,20] and amplifies the activity of extracellular stimuli.[21,22]

Vasculature may be a target of GAS6/Axl axis, being both molecules expressed by endothelial cells (ECs),[4,9] pericytes,[23] and smooth muscle cells.[24] GAS6/Axl interaction is involved in leukocyte transmigration through capillaries,[4,8] in neointima formation in injured vessels,[24] and in EC survival after tumor necrosis factor α (TNF-α) treatment or acidification.[16,18] Mice lacking the 3 tyrosine kinase receptors, which bind GAS6, show alteration in vasculature survival.[6]

By activating specific and partially overlapping genetic programs, ECs play key roles in many processes, as regulation of vascular tone, lipid metabolism, hematopoiesis, inflammation, antigen recognition, thrombosis, hemostasis, and angiogenesis.[25] Angiogenesis refers to the remodeling and maturation of the primitive vascular plexus formed by vasculogenesis during the development and to the sprouting and subsequent stabilization by pericytes of new capillaries from preexisting ones in adult life.[26] Physiologic angiogenesis results from a fine-tuning balance between inducers and inhibitors and achieves a network hierarchically and spatially organized to provide adequate nutrients to the cells. When this balance is perturbed, vessel growth is deregulated

From the Department of Anatomy, Pharmacology, and Forensic Medicine, University of Turin, Torino, Italy; the Division of Molecular Angiogenesis, Institute for Cancer Research and Treatment (IRCC), School of Medicine, University of Turin, Candiolo, Italy; the Department of Oncological Science, University of Turin, Torino, Italy; Amgen Inc, Amgen Center, Thousand Oaks, California; and the Department of Medical Science, University "Amedeo Avogadro," Novara, Italy.

Submitted April 16, 2004; accepted October 14, 2004. Prepublished online as *Blood* First Edition Paper, October 26, 2004; DOI 10.1182/blood-2004-04-1469.

Supported by Associazione Italiana per la Ricerca sul Cancro, Istituto Superiore di Sanità (Progetto "Tumor therapy"), Ministero dell' Università e della Ricerca (MIUR) (60% and Progetti di Rilevauza e Interesse Nazionale [PRIN] 2002 projects), Centro Nazionale delle Ricerche-MIUR. (Progetto Strategico Oncologia), and Fondi incentivazione della Ricerca di Base. F.B. belongs to the European Vascular Genomics Network (http://www.engv.org) supported by European Community (contract LSHM-CT-2003-503254).

One of the authors (B.V.) is employed by Amgen whose product was studied in the present work and could be of commercial interest.

Reprints: Margherita Gallicchio, Department of Anatomy, Pharmacology and Forensic Medicine, C. so Massimo D'azeglio 52, 10100 Torino, Italy; e-mail: margherita.gallicchio@unito.it.

The publication costs of this article were defrayed in part by page charge payment. Therefore, and solely to indicate this fact, this article is hereby marked "advertisement" in accordance with 18 U.S.C. section 1734.

with formation of aberrant and physiologically immature capillaries, contributing to the pathogenesis of many disorders.[27,28] On a molecular point of view, vessel growth and maturation are highly complex and coordinated processes, which require the sequential activation of a broad variety of membrane receptors by specific ligands. In this context, vascular endothelial growth factor (VEGF)–A often represents a rate-limiting step for physiologic vascular network formation and also seems to be extremely important in disease-associated angiogenesis.[29] VEGF-A binds to and activates 2 tyrosine kinase receptors, VEGF receptor (R)–1 and VEGFR-2, being the later the principal target of VEGF-A in adult life.[29]

Here, we investigate the role of GAS6/Axl axis in angiogenesis, showing that this axis may inhibit VEGFR-2 dependent activation of ECs.

Materials and methods

Cells

Human ECs were isolated from umbilical cord veins, characterized and grown in M199 medium (Sigma-Aldrich, St Louis, MO) containing 20% fetal calf serum (FCS) as previously reported.[30] They were used at early passages (I-IV). To infect ECs[31] cDNAs of SHP-2 (SH2 domain-containing tyrosine phosphatase 2) C/S, in which Cys 459 is substituted by Ser,[32] were subcloned into the *Bam*HI/*Eco*RI site of a modified Pinco retroviral vector[33] and was expressed under the control of the 2 long terminal repeats. Green fluorescence protein (GFP) cDNA was under the control of cytomegalovirus promoter. As control of infection, GFP analysis was performed both through fluorescence microscope and fluorescence-activated cell sorting (FACS Advantage SE; BD Biosciences, Mountain View, CA) giving 85% to 90% of positive ECs. The expression of transgene molecules was evaluated by Western blot analysis by specific antibody (Ab) anti–SHP-2 (Santa Cruz Biotechnology, Santa Cruz, CA). Infection conditions did not modify EC shape and cell cycle, which was analyzed by propidium iodide fluorescence with fluorescence activated cell sorter laboratory (FACS) flow cytometer.

Cell chemotaxis

Chemotaxis assays were performed as previously described[30] by the Boyden chamber technique (AP48 micro chemotaxis chamber; Neuroprobe, Pleasanton, CA) using a 5-μm pore size polycarbonate filter (Neuroprobe) coated on both sides with gelatin (0.1% for 6 hours at room temperature). VEGF-A_{165}, VEGF-A_{121}, fibroblast-growth factor 2 (FGF-2), or hepatocyte growth factor (HGF) (R&D Systems, Minneapolis, MN) in the presence or absence of GAS6[12] in M199 supplemented with 0.25% bovine serum albumin were seeded in the lower compartment of the chamber, and 2×10^5 suspended cells in M199 containing 1% FCS were then seeded in the upper compartment. After 5 hours of incubation at 37°C with 5% CO_2, the upper surface of the filter was scraped with a rubber policeman. The filters were fixed and stained with Diff-Quick (Baxter Spa, Rome, Italy), and 10 fields were counted after coding samples at 400 × magnification. In preliminary experiments, the minimal amount of angiogenic inducers giving the maximal chemotactic response was established. Therefore, all experiments were performed with VEGF-A_{165}, VEGF-A_{121}, and HGF used at 10 ng/mL, and FGF-2 at 20 ng/mL. In experiments performed in the presence of Axl inhibitors, ECs were preincubated for 30 minutes with 5 μg/mL Axl-immunoglobulin (Ig) or an Ab anti-Axl[12] at 37°C with 5% CO_2. As control, nonimmune rabbit Ig (Sigma-Aldrich) was used and did not show any activity.

In vitro morphogenesis assay

Matrigel (growth factor–free; BD Biosciences) was added to each well of a 48-well plate and incubated at 37°C for 30 minutes to allow gel formation. ECs (2×10^4/well) were plated onto Matrigel in M199 containing 0.5% FCS and treated as indicated. After 12-hour incubation in 5% CO_2 humidified atmosphere at 37°C, the cell 3-dimensional organization was examined under DM-IBM inverted-phase contrast photomicroscope (objective: 5 ×/0.12; medium: AIR; Leica Microsystem, Heerbrugg, Switzerland) and then photographed.[34] Capillary-like structures were quantified[35] by automatic counting in triplicate of low-power fields (× 40) using the ImageProPlus 4.0 imaging software (Media Cybernetics, Leiden, The Netherlands), and percentage variation was expressed assuming VEGF-A_{165}–treated ECs as 100%.

Chick embryo chorioallantoic membrane (CAM) assay

Fertilized white Leghorn chick eggs were incubated under conditions of constant humidity at 37°C. On the third day of incubation, a square window was opened in the eggshell after removal of 2 to 3 mL albumen so as to detach the developing CAM from the shell. The window was sealed with a glass of the same size, and the eggs were returned to the incubator. At day 8, 1-mm^3 sterilized gelatin sponges (Gelfoam; Upjohn, Kalamazoo, MI) adsorbed with the indicated molecules dissolved in 3 μL phosphate-buffered saline were implanted on the top of growing CAMs.[36] CAMs were examined daily until day 12 when they were photographed in ovo under a Zeiss stereomicroscope SR equipped with an MC 63 Camera System (Zeiss, Oberkochen, Germany). The number of vessels was quantified with ImageProPlus 4.0 imaging software in 3 randomly selected areas (1 mm^2) as previously described.[37]

Immunoprecipitation and immunoblotting

Confluent ECs (1×10^7 cells/150 cm^2 dish) were made quiescent by 20 hours of starvation in M199 containing 0.5% FCS and 0.1% human serum albumin (Farma Biagini, Lucca, Italy), preincubated for 15 minutes at 37°C with 1 mM Na_3V0_4 and then stimulated as indicated. Proteins were alternatively immunoprecipitated with monoclonal antibody (mAb) antiphosphotyrosine (anti–P-Tyr; Upstate Biotechnology, BD Biosciences), Ab anti–VEGFR-2 (R&D Systems and Santa Cruz), Ab anti-Axl[12] exactly as previously described.[38] Proteins were solubilized in reducing conditions, separated by sodium dodecylsulfate (SDS)–polyacrilamide gel electrophoresis (PAGE) (8% or 10%), transferred to Immobilon-P sheets (Millipore, Bedford, MA) and probed with specific and indicated Abs. The enhanced chemiluminescence technique (New England Nuclear [NEN]; Perkin Elmer, Cetus, Norwalk, CT) was used for detection.

Binding displacement assay

The binding of VEGF-A_{165} with its high-affinity sites on ECs reaches the equilibrium after 90 minutes at room temperature.[39] On the basis of these data, binding displacement studies with GAS6 were performed. Cell monolayers on 24-well plates were incubated for 90 minutes at room temperature in 0.2 mL M199 containing 20 mM HEPES (*N*-2-hydroxyethylpiperazine-*N*′-2-ethanesulfonic acid), pH 7.4, 0.1% bovine serum albumin, 100 μg/mL soybean trypsin inhibitor (Sigma-Aldrich) with 0.05 nM [^{125}I] VEGF-A (specific activity 140 μCi/μg [5.18 MBq]; Amersham-Biotech-Pharmacia, Milano, Italy) and increasing concentrations of cold GAS6 or VEGF-A_{165}. The cells were washed twice with phosphate-buffered saline, solubilized with SDS 2% in phosphate-buffered saline, and the radioactivity was counted.

Results

GAS6 activates Axl receptor and inhibits VEGF-A–dependent chemotaxis of ECs

Stimulation of EC motility is a necessary and, in some cases, sufficient step of vascular pattern formation.[40-42] Therefore, we examined the effect of GAS6 on in vitro EC chemotaxis. GAS6 was ineffective in promoting EC directional migration but consistently inhibited in a dose-dependent fashion the chemotactic effect of optimal concentration of VEGF-A_{165} and VEGF-A_{121} (Figure 1A). GAS6 (1 ng/mL) inhibited at 50% the chemotaxis induced by

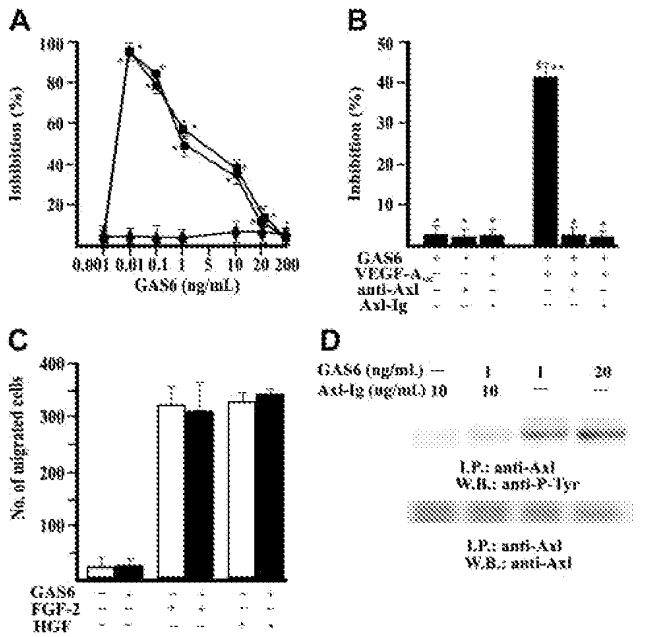

Figure 1. GAS6 modulates VEGF-A–induced EC chemotaxis through activation of Axl. (A) EC chemotaxis was evaluated in presence of GAS6 alone (◆) or associated with VEGF-A_{165} (●) or VEGF-A_{121} (■) (10 ng/mL). Results of 1 experiment performed in triplicate representative of 3 independent experiments are shown. Data are presented as percentage of inhibition of VEGF-A_{165} (403 ± 34 cells/microscopic field) or VEGF-A_{121} (389 ± 24 cells/microscopic field) induced chemotaxis. Results were analyzed by 1-way analysis of variance (ANOVA) (F = 287.28) and Student-Newman-Keuls test. $^*P < .05$ versus stimulated cells in absence of GAS6. (B) Chemotaxis of ECs in presence of Ab anti–Axl-N or Axl-Ig. Results of 1 experiment performed in triplicate representative of 4 independent experiments are shown. Data were analyzed by ANOVA (F = 7.93) and Student-Newman-Keuls test. $^*P < .05$ versus GAS6 (1 ng/mL) alone; $^{**}P < .05$ versus GAS6 + anti–Axl-N; §$P < .05$ versus GAS6 + Axl-Ig. (C) Effect of GAS6 (1 ng/mL) on FGF-2 (20 ng/mL) and HGF (10 ng/mL) induced EC chemotaxis. □ indicates absence, ■ presence of GAS6. (D) Axl phosphorylation by GAS6. Quiescent, confluent ECs were stimulated for 30 minutes as indicated at 37°C with 5% CO_2. Cells were lysated and immunoprecipitated for 2 hours at 4°C with an anti-Axl Ab. Immunoprecipitate was analyzed by sodium dodecyl sulfate-polyacrilamide gel electrophoresis (SDS-PAGE) followed by immunoblotting with anti–P-Tyr mAb or an anti-Axl Ab. Immunoreactive bands were detected by enhanced chemiluminescence technique. I.P. indicates immunoprecipitate; W.B., Western blot. The results are representative of 4 similar experiments. Error bars in A-C indicate standard deviation.

10 ng/mL VEGF-A_{165} and was used in successive experiments. The presence in the chemotaxis assay of a soluble immunoglobulin fusion protein containing the Axl extracellular domain (Axl-Ig) or a polyclonal Ab directed toward the N-terminus extremity of Axl (αAxl-N)[12] blocked the effect of GAS6, demonstrating that Axl is the RTK engaged by GAS6 (Figure 1B). GAS6 used at 1 ng/mL (Figure 1C) or at higher concentrations (from 10 ng/mL up to 500 ng/mL) (not shown) did not influence the chemotactic activity of FGF-2 and HGF, suggesting that it specifically inhibits the effect of VEGF-A. GAS6 induced the autophosphorylation in tyrosine residues of Axl immunoprecipitated from ECs, being active at 1 ng/mL. This activity was abolished by the presence of the decoy receptor Axl-Ig (Figure 1D).

GAS6 inhibits the autonomous property of ECs to form capillary-like networks

ECs cultured on Matrigel, a natural basal membrane matrix, spontaneous differentiate in geometric tubular networks independently from cell mitosis.[42] This process requires directed cell migration governed by the presence of VEGF-A, which mainly acts in paracrine/autocrine manner, as inferred by the inhibitory effect

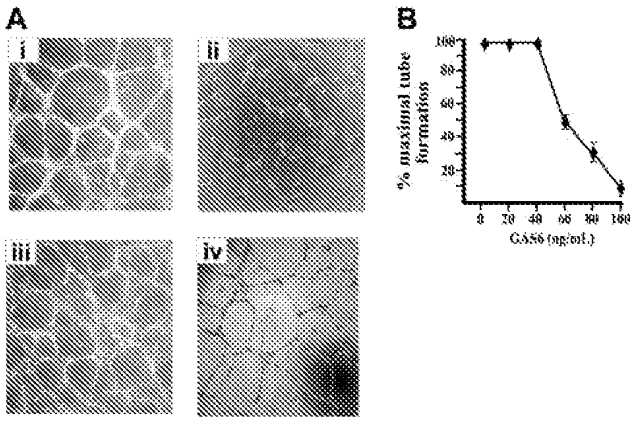

Figure 2. EC morphogenesis on Matrigel is modulated by GAS6. (A) Morphologic aspect of ECs plated on Matrigel for 12 hours in the presence of M199 containing 0.5% FCS (i) supplemented with GAS6 (100 ng/mL) (ii), GAS6 in the presence of Axl-Ig (1 μg/mL) (iii), or Axl-Ig alone (iv). Pictures are representative of 5 independent experiments. Images were processed by Image Proplus 4.0 (Media Cybernetycs, Leiden, The Netherlands). (B) Dose-dependent inhibition of EC morphogenesis by GAS6. Tubular structures were quantified by automatic counting of tube formation after 12 hours. Percentage of inhibition was expressed using untreated GAS6 cells as 100%. Mean ± SD of 4 experiments.

exerted by an Ab anti–VEGF-A.[42] As shown in Figure 2, the presence of GAS6 impaired the morphogenetic potential of ECs on Matrigel in a dose-dependent manner, and the maximal inhibitory effect was obtained at 80 to 100 ng/mL (Figure 2B). In the presence of GAS6, ECs were unable to form cords interconnected with nodes and remained mostly sparse with few chains formed. The addition of Axl-Ig reverted the GAS6 effect, while Axl-Ig alone was ineffective (Figure 2A).

GAS6 inhibits VEGF-A–dependent vascularization in CAM assay

The in vivo inhibitory effect of GAS6 on vascular formation was demonstrated in the CAM assay (Figure 3; Table 1). The gelatin sponges treated with VEGF-A_{165} (50 ng) were surrounded by allantoic vessels radiating toward the implant in a spoked-wheel pattern (Figure 3A), while GAS6 used at 50 ng/sponge was ineffective (Figure 3B). GAS6 did not promote vascularization in a range from 1 ng to 500 ng (data not shown). In contrast, GAS6 used at 20 ng/sponge was able to inhibit the activity of VEGF-A_{165}

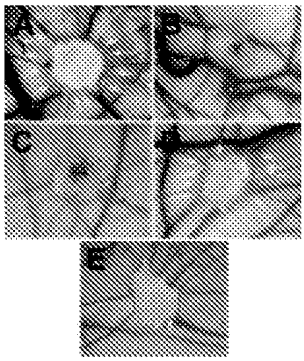

Figure 3. GAS6 inhibits VEGF-A_{165}–mediated vascularization in CAM assay. CAMs were recorded at day 12 of incubation, 96 hours after the implant of a gelatin sponge soaked with VEGF-A_{165} (50 ng) (A), GAS6 (50 ng) (B), VEGF-A_{165} with GAS6 (20 ng) (C), or phosphate-buffered saline (E). Panel D shows the reverting effect of the presence Axl-Ig (200 ng) on the inhibitory effect of GAS6 (20 ng). Arrows in panels A and D indicate the new capillaries attracted by the sponges. Original magnification × 50. The picture is representative of 1 experiment of at least 4 performed. Images were processed by Image Proplus 4.0.

Table 1. Angiogenic effects of GAS6 and Axl-Ig on the chick CAM

Stimulation	No. of CAM examined	Vessel/mm³*	Statistical significance†
Vehicle	10	4.58 ± 1.16	‡
VEGF-A_{165}§	10	14.46 ± 2.52	¶
VEGF-A_{165} + GAS6	5	7.03 ± 0.47	‡¶
FGF-2	5	16.32 ± 1.26	¶
FGF-2 + GAS6	6	15.50 ± 2.12	¶
VEGF-A_{165} + GAS6 + Axl-Ig	3	12.14 ± 2.62	¶
GAS6	4	4.00 ± 0.62	‡
GAS6 + Axl-Ig	4	4.21 ± 1.63	‡
Axl-Ig	4	4.14 ± 1.43	‡

*Images photographed as described in "Materials and methods" were digitally recorded, and the number of vessels was quantified with an imaging software in 3 randomly selected areas (1 mm³).

†Data were analyzed by ANOVA ($F = 31.29$) and Student-Newman-Keuls test.

‡$P < .05$ within indicated stimulations and CAM stimulated by VEGF-A_{165}.

§VEGF-A_{165} or FGF-2, GAS6, and Axl-Ig were used at 50 ng, 20 ng, and 200 ng per sponge, respectively.

¶$P < .05$ within indicated stimulations and CAM stimulated by vehicle alone.

(Figure 3C; Table 1) but not that of FGF-2 (Table 1). VEGF-A_{165} induced angiogenesis in the presence of the decoy receptor Axl-Ig, supporting the direct involvement of GAS6-Axl axis in the control of the vascularization mediated by VEGF-A (Figure 3D; Table 1).

GAS6 inhibits autophosphorylation of VEGFR-2 induced by VEGF-A

Autophosphorylation in tyrosine residues is the earliest event occurring after VEGF-A–dependent VEGFR-2 dimerization.[29] To explore the mechanism by which GAS6 affected VEGF-A activities, VEGFR-2 was immunoprecipitated from ECs and analyzed for its phosphorylation state. Figure 4 shows that a short preincubation of ECs with GAS6 at 1 ng/mL resulted in a marked inhibition of VEGFR-2 autophosphorylation. To evaluate a possible cross talk between VEGFR-2 and Axl, ECs were stimulated as in the previous experiment, and the lysates were immunoprecipitated with a mAb anti–P-Tyr. As shown in Figure 4B, the presence of VEGF-A_{165} did not affect Axl phosphorylation.

To exclude that the observed inhibition of VEGFR-2 phosphorylation may be the consequence of a competitive mechanisms, we studied the effect of GAS on the binding of [^{125}I] VEGF-A_{165} on ECs. In Figure 5, the preincubation of ECs with increasing concentrations of GAS6 did not inhibit the binding of labeled VEGF-A_{165}. Therefore, GAS6 did not interfere in the binding of

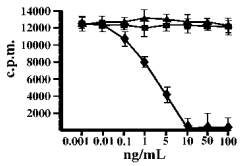

Figure 5. Effect of GAS6 on the binding of [^{125}I]VEGF-A_{165} at equilibrium to ECs. Cell monolayers were incubated for 90 minutes at room temperature in 0.2 mL binding buffer with 0.05 nM [^{125}I] VEGF-A without (■) or with the indicated concentrations of unlabeled VEGF-A_{165} (◆), and GAS6 (●). At the end of incubation, the cells were washed and solubilized with SDS 2%, and the radioactivity was counted. Data are the mean ± SD of 3 determinations in 1 experiment of 2 with similar results

VEGF-A_{165} to its specific affinity sites. In contrast, cold VEGF-A_{165} inhibited the binding of [^{125}I] VEGF-A to ECs with an apparent IC_{50} (inhibitory concentration 50%) of 60 pM as shown in other reports (reviewed in Thomas[43]).

Tyrosine phosphatase SHP-2 is involved in the inhibitory activity of GAS6 on VEGF-A–mediated EC activation

It is well established that cytosolic protein tyrosine phosphatases containing src homology domain-2 regulate intracellular pathways activated by several receptors including RTK.[44,45] SHP-2 has been implicated in the signaling pathways triggered by VEGF-A,[46] and our preliminary results indicate that it dephosphorylates VEGFR-2 in vitro (S.M., F.B., in preparation). Therefore, we tested the hypothesis that SHP-2 could be responsible of the inhibitory signal mediated by GAS6-Axl axis on VEGF-A activities. GAS6 induces tyrosine phosphorylation of SHP-2 (Figure 6A) and its association with Axl (Figure 6B-C), suggesting the activation of its catalytic property.[45] The phosphorylation occurred within 5 minutes and persisted up to 30 minutes.

Therefore, ECs were infected with a retroviral vector carrying SHP-2 C/S, the catalytically inactive Cys-to-Ser mutant form[47] (Figure 2A). The expression of this mutant did not modify the GAS6-dependent Axl phosphorylation. (Figure 7B). Furthermore, the expression of SHP-2 C/S mutant was able to suppress SHP-2 phosphorylation triggered by GAS6. This is a surprising result because the point mutation in SHP-2 C/S does not involve the SH-2 domain; therefore, the enzyme may associate to Axl. It is possible that the relative amount of SHP-2 phosphorylated by endogenous levels of Axl tyrosine kinase is reduced and not detected by immunoprecipitation followed by immunoblotting, due to the high

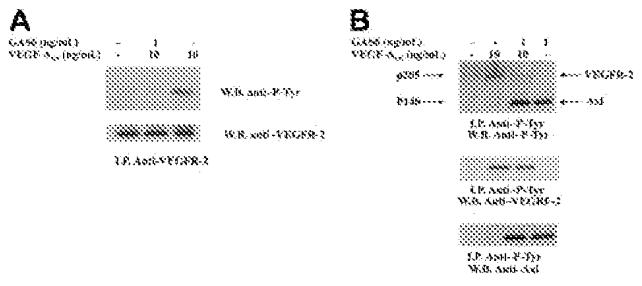

Figure 4. Inhibition of VEGFR-2 phosphorylation by GAS6. ECs were preincubated with GAS6 (1 ng/mL) for 20 minutes and consequently stimulated for 10 minutes with VEGF-A_{165} (10 ng/mL). Cell lysates were immunoprecipitated with an anti–VEGFR-2 Ab, analyzed by SDS-PAGE, followed by immunoblotting with the indicated Abs. The results are representative of 4 similar experiments. (B) ECs were preincubated with GAS6 (1 ng/mL) for 20 minutes and consequently stimulated for 10 minutes with VEGF-A_{165} (10 ng/mL). Cell lysates were immunoprecipitated with an anti–P-Tyr, analyzed by SDS-PAGE, followed by immunoblotting with the indicated Abs. The results are representative of 4 similar experiments.

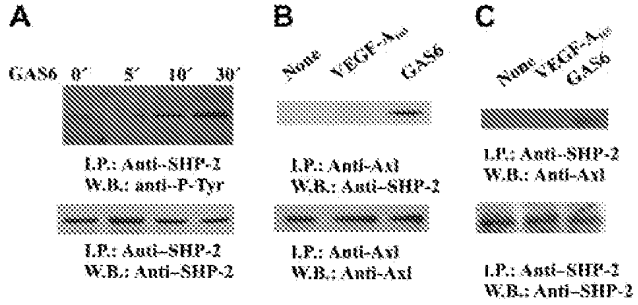

Figure 6. GAS6 activates SHP-2. (A) SHP-2 activation by GAS6. Quiescent, confluent ECs were stimulated for the indicated times with GAS6 (1 ng/mL), and cell lysates were immunoprecipitated by Ab anti–SHP-2. Immunodetection was performed with Ab anti–P-Tyr or anti–SHP-2. (B-C) GAS6 mediates SHP-2 association with Axl. Quiescent, confluent ECs were stimulated for 30 minutes with GAS6 (1 ng/mL), and cell lysates were immunoprecipitated by Ab–anti-Axl (B) or anti–SHP-2 (C). (C) Immunoprecipitate was divided into 2 aliquots. Immunodetection was performed as indicated. The results are representative of 3 similar experiments.

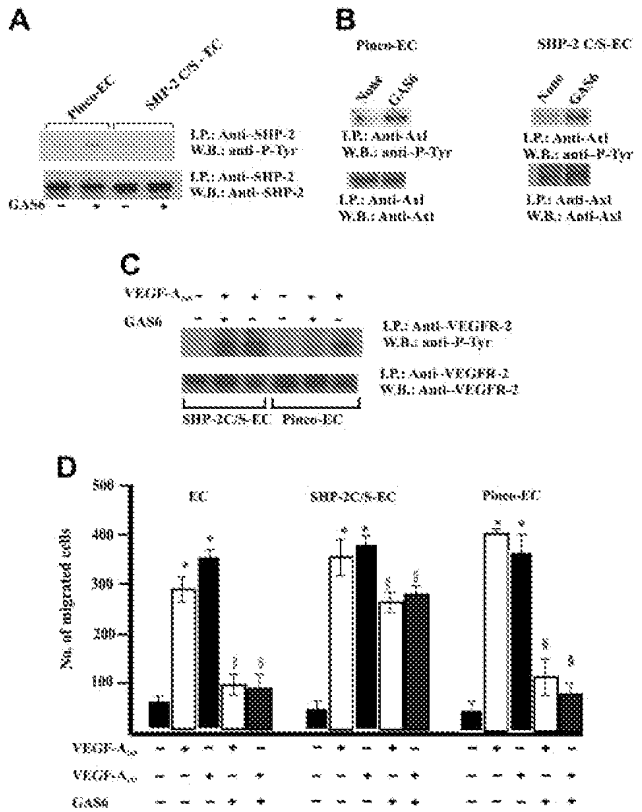

Figure 7. Expression of SHP-2 C/S mutant inhibits GAS6 modulation of EC chemotaxis induced by VEGF-A_{165}. (A) Effect of SHP-2 C/S expression on Tyr phosphorylation of SHP-2. Quiescent, confluent infected ECs were stimulated for 30 minutes with GAS6 (1 ng/mL). Cell lysates were immunoprecipitated with Ab anti–SHP-2 and immunoblotted with the same Ab or with Ab anti–P-Tyr. (B) Effect of SHP-2 C/S expression on Tyr phosphorylation of Axl. Pinco-ECs and SHP-2 C/S-ECs were stimulated with GAS6 (1 ng/mL for 30 minutes). Immunoprecipitation was performed with Ab anti-Axl, and proteins were immunodetected with Ab anti–P-Tyr or anti-Axl. (C) Effect of SHP-2 C/S expression on Tyr phosphorylation of VEGFR-2. Pinco-ECs and SHP-2 C/S-ECs were preincubated with GAS6 (1 ng/mL) for 20 minutes and consequently stimulated for 10 minutes with VEGF-A_{165} (10 ng/mL). Immunoprecipitation was performed with Ab anti–VEGFR-2, and proteins were immunodetected with Ab anti–P-Tyr or anti–VEGFR-2. (D) EC chemotaxis induced by VEGF-A_{165} and VEGF-A_{121} (both at 10 ng/mL) was evaluated in cells infected with vector alone, or carrying SHP-2 C/S mutant or SHP-2. When indicated 1 ng/mL GAS6 was added. Results of 1 experiment performed in triplicate representative of 3 independent experiments are shown. Data were analyzed by ANOVA ($F = 495.89$ for SHP-2, $F = 876.7$ for SHP-2 C/S) and Student-Newman-Keuls test. $^*P < .05$ versus control; $\S P < .05$ versus VEGF-A_{165} or VEGF-A_{121} alone.

expression levels of SHP-2 obtained by the efficiency of retroviral infection as compared with the endogenous enzyme levels.

An essential confirmation of the role of this phosphatase as effector of GAS6 on VEGFR-2 was inferred by the lack of inhibition of VEGFR-2 phosphorylation in ECs expressing SHP-2 C/S and stimulated by VEGF-A_{165} (Figure 7C). Figure 7D shows that GAS6 inhibited EC chemotaxis induced by VEGF-A_{121} and VEGF-A_{165}. The expression of the SHP-2 mutant abrogated this effect, substantiating that this phosphatase is involved with the negative signaling exerted by GAS6 on VEGF-A.

Discussion

GAS6 has been reported to have a broad range of activities in different contexts. The differences usually depend on the cell type studied and the concentration used.[4,5,13-20] It induces migration of smooth muscle cells and inhibits neutrophil adhesion to ECs.[4,20] High concentrations of GAS6 (100-800 ng/mL) inhibit EC apoptosis.[4,16,18] Furthermore it affects the response of blood vessels to injury, thereby contributing to the development of restenosis/atherosclerosis.[48] Finally, GAS6 has been detected in inflammatory diseases[18,49] and in human cancers.[50,51]

In the present study we describe a GAS6-dependent inhibitory pathway, which selectively hinders the angiogenic program activated by VEGF-A. Through Axl RTK, GAS6 activates the tyrosine phosphatase SHP-2, which, in turn, down-regulates signals starting from VEGFR-2. This statement is based on the following data: (1) GAS6 inhibits the chemotaxis stimulated by VEGF-A, while it is ineffective when ECs are stimulated by FGF-2 or HGF; (2) it inhibits in vitro EC morphogenesis in a model in which vascular pattern formation is mainly driven by the autocrine/paracrine effect of VEGF-A,[42] as well CAM vascularization stimulated by VEGF-A, but not by FGF-2; (3) it inhibits the VEGF-A–dependent phosphorylation of VEGFR-2; (4) it triggers Axl receptor, which, in turn, recruits SHP-2 in an active form to its cytosolic tail; (5) the overexpression of a dominant-negative mutant of SHP-2 does not inhibit Axl activation, but specifically abrogates EC chemotaxis as well as VEGFR-2 phosphorylation promoted by VEGF-A.

Cross talk between RTKs[52-54] enable cells to integrate signals from different stimuli, thereby coordinating and refining complex responses. Through a SHP-2–dependent negative transmodulation of VEGFR-2, the GAS6/Axl axis controls the motility potential of VEGF-A. Therefore, the inhibitory signal exerted by GAS6 may finely balance the highly positive effect of VEGF-A on EC motility, resulting in a proper alignment of cells required to establish a well-shaped vascular pattern. It is intriguing to highlight that GAS6 may be produced by pericytes,[23] which are of critical importance for vascular morphogenesis dictating vascular sprouting in some tissue.[55,56] This scenario evocates other environmental cues that negatively regulate cell migration by directly interfering with integrin-mediated outside-in signals involved in cytoskeletal organization and propulsive force generation.[42,57] In this context, the known antiapoptotic effect of GAS6 in ECs[16,18] may participate in survival mechanisms required for cells to successfully migrate.[57] Migrating cells lose their integrin-mediated contacts with the extracellular matrix and therefore could undergo an apoptotic program (anoikisis) that may be differently counteracted by signals, including those triggered by GAS6. The apparent paradox of an antiapoptotic factor that contributes in inhibiting angiogenesis is supported by recent findings on fortilin.[58] This is a nuclear antiapoptotic factor, which inhibits migration of smooth muscle cells in vitro. In experimental angioplasty fortilin reduces neointima formation through powerful antiproliferative and antimigratory actions concomitant with the ability to reduce vascular cell apoptosis and maintain vessel integrity.[58]

The tyrosine phosphatase SHP-2 is widely expressed and can both positively or negatively regulate intracellular signals generated by RTKs, G-protein–associated receptors, and cytokine receptors.[59-67] Our results of the dominant-negative mutant of SHP-2 reverting the inhibitory effects of GAS6 suggest an involvement of this phosphatase activated by GAS6 in inhibiting VEGF-A action. This observation parallels the results that VEGFR-2 may be negatively regulated by tumor necrosis factor-α or by tissue inhibitor of metalloproteinases-2 (TIMP-2) through SHP-1.[68,69] The present study does not investigate the precise mechanism by which VEGFR-2 is inactivated by GAS6. It is intriguing to speculate on a direct effect of SHP-2 on VEGFR-2. In ECs stimulated by TIMP-2, SHP-1 dephosphorylates VEGFR-2 by shifting from α3β1 integrin to the receptor.[69] Alternatively, we may

hypothesize an indirect effect mediated by other tyrosine phosphatases, including human low–molecular-weight cytoplasmic protein tyrosine phosphatase (HCPTPA), which specifically dephosphorylates VEGFR-2.[70]

Our results cannot exclude that the observed effects of SHP-2 in GAS6–dependent inhibition of EC motility exclusively occurs by interfering VEGFR-2–triggered signals. Actually cells derived from SHP-$2^{-/-}$ mice or expressing a SHP-2 dominant-negative mutant display severe defects in spreading, haptotactic, and chemotactic response,[71-73] being that this phosphatase is involved in adhesion dynamics.[53,74]

A large number of strategies occur to counteract the effect of angiogenic inducers, and a right balance between inhibitors and agonists is instrumental in formation of an accurate vasculature in embryonic and adult tissues.[27,75] With the exception of decoy receptors that antagonize selected agonists,[76] inhibition of angiogenesis occurs by impairing general function of ECs (ie, migration, survival, proliferation) independently from stimuli.[75,77,78] Our results suggest that GAS6-Axl axis represents a specific inhibitory pathway for VEGF-A–mediated angiogenesis. Interfering in VEGF-A–mediated signals seems to be the first promising application of antiangiogenic therapy in human cancers.[79,80] Therefore, delineation of a selective mechanism that turns off VEGFR-2 may facilitate the design of further and effective combination therapies for disruption of vascular network in tumors. However, in the light of limited knowledge on the role played by GAS in human and experimental diseases, our results need further validations in specific animal models.

Acknowledgments

We thank Dr J. Zhao (Vanderbilt University, Nashville, TN) for providing SHP-2 mutant and Dr E. Giraudo (University of Torino, Italy) for his criticisms.

References

1. O'Bryan JP, Frye RA, Cogswell PC, et al. axl, a transforming gene isolated from primary human myeloid leukemia cells, encodes a novel receptor tyrosine kinase. Mol Cell Biol. 1991;11:5016-5031.
2. Lai C, Gore M, Lemke G. Structure, expression, and activity of Tyro 3, a neural adhesion-related receptor tyrosine kinase. Oncogene. 1994;9:2567-2578.
3. Graham DK, Dawson TL, Mullaney DL, Snodgrass HR, Earp HS. Cloning and mRNA expression analysis of a novel human protooncogene, c-mer. Cell Growth Differ. 1994;5:647-657.
4. Avanzi GC, Gallicchio M, Bottarel F, et al. GAS6 inhibits granulocyte adhesion to endothelial cells. Blood. 1998;91:2334-2340.
5. Nakano T, Kawamoto K, Kishino J, Nomura K, Higashino K, Arita H. Requirement of gamma-carboxyglutamic acid residues for the biological activity of Gas6: contribution of endogenous Gas6 to the proliferation of vascular smooth muscle cells. Biochem J. 1997;323:387-392.
6. Lu Q, Gore M, Zhang Q, et al. Tyro-3 family receptors are essential regulators of mammalian spermatogenesis. Nature. 1999;398:723-728.
7. Bellosta P, Costa M, Lin DA, Basilico C. The receptor tyrosine kinase ARK mediates cell aggregation by homophilic binding. Mol Cell Biol. 1995;15:614-625.
8. Lu W, Lemke G. Homeostatic regulation of the immune system by receptor tyrosine kinases of the Tyro 3 family. Science. 2001;293:306-311.
9. Manfioletti G, Brancolini C, Avanzi G, Schneider C. The protein encoded by a growth arrest-specific gene (gas6) is a new member of the vitamin K-dependent proteins related to protein S, a negative coregulator in the blood coagulation cascade. Mol Cell Biol. 1993;13:4976-4985.
10. Ohashi K, Nagata K, Toshima J, et al. Stimulation of sky receptor tyrosine kinase by the product of growth arrest-specific gene 6. J Biol Chem. 1995;270:22681-22684.
11. Nagata K, Ohashi K, Nakano T, et al. Identification of the product of growth arrest-specific gene 6 as a common ligand for Axl, Sky, and Mer receptor tyrosine kinases. J Biol Chem. 1996;271:30022-30027.
12. Varnum BC, Young C, Elliott G, et al. Axl receptor tyrosine kinase stimulated by the vitamin K-dependent protein encoded by growth-arrest-specific gene 6. Nature. 1995;373:623-626.
13. McCloskey P, Fridell YW, Attar E, et al. GAS6 mediates adhesion of cells expressing the receptor tyrosine kinase Axl. J Biol Chem. 1997;272:23285-23291.
14. Yanagita M, Arai H, Nakano T, et al. Gas6 induces mesangial cell proliferation via latent transcription factor STAT3. J Biol Chem. 2001;276:42364-42369.
15. Bellosta P, Zhang Q, Goff SP, Basilico C. Signaling through the ARK tyrosine kinase receptor protects from apoptosis in the absence of growth stimulation. Oncogene. 1997;15:2387-2397.
16. D'Arcangelo D, Gaetano C, Capogrossi MC. Acidification prevents endothelial cell apoptosis by Axl activation. Circ Res. 2002;91:e4–12.
17. Goruppi S, Ruaro E, Varnum B, Schneider C. Gas6-mediated survival in NIH3T3 cells activates stress signalling cascade and is independent of Ras. Oncogene. 1999;18:4224-4236.
18. O'Donnell K, Harkes IC, Dougherty L, Wicks IP. Expression of receptor tyrosine kinase Axl and its ligand Gas6 in rheumatoid arthritis: evidence for a novel endothelial cell survival pathway. Am J Pathol. 1999;154:1171-1180.
19. Allen MP, Linseman DA, Udo H, et al. Novel mechanism for gonadotropin-releasing hormone neuronal migration involving Gas6/Ark signaling to p38 mitogen-activated protein kinase. Mol Cell Biol. 2002;22:599-613.
20. Fridell YW, Villa J Jr, Attar EC, Liu ET. GAS6 induces Axl-mediated chemotaxis of vascular smooth muscle cells. J Biol Chem. 1998;273:7123-7126.
21. Angelillo-Scherrer A, de Frutos P, Aparicio C, et al. Deficiency or inhibition of Gas6 causes platelet dysfunction and protects mice against thrombosis. Nat Med. 2001;7:215-221.
22. Nakano T, Higashino K, Kikuchi N, et al. Vascular smooth muscle cell-derived, Gla-containing growth-potentiating factor for Ca(2+)-mobilizing growth factors. J Biol Chem. 1995;270:5702-5705.
23. Collett G, Wood A, Alexander MY, et al. Receptor tyrosine kinase Axl modulates the osteogenic differentiation of pericytes. Circ Res. 2003;92:1123-1129.
24. Melaragno MG, Wuthrich DA, Poppa V, et al. Increased expression of Axl tyrosine kinase after vascular injury and regulation by G protein-coupled receptor agonists in rats. Circ Res. 1998;83:697-704.
25. Mantovani A, Bussolino F, Introna M. Cytokine regulation of endothelial cell function: from molecular level to the bedside. Immunol Today. 1997;18:231-239.
26. Carmeliet P. Mechanisms of angiogenesis and arteriogenesis. Nat Med. 2000;6:389-395.
27. Hanahan D, Folkman J. Patterns and emerging mechanisms of the angiogenic switch during tumorigenesis. Cell. 1996;86:353-364.
28. Jain RK. Molecular regulation of vessel maturation. Nat Med. 2003;9:685-693.
29. Ferrara N, Gerber HP, LeCouter J. The biology of VEGF and its receptors. Nat Med. 2003;9:669-676.
30. Bussolino F, Di Renzo MF, Ziche M, et al. Hepatocyte growth factor is a potent angiogenic factor which stimulates endothelial cell motility and growth. J Cell Biol. 1992;119:629-641.
31. Primo L, Roca C, Ferrandi C, Lanfrancone L, Bussolino F. Human endothelial cells expressing polyoma middle T induce tumors. Oncogene. 2000;19:3632-3641.
32. Zhao Z, Tan Z, Wright J, et al. Altered expression of protein-tyrosine phosphatase 2C in 293 cells affects protein tyrosine phosphorylation and mitogen-activated protein kinase activation. J Biol Chem. 1995;270:11765-11769.
33. Cutrupi S, Baldanzi G, Gramaglia D, et al. Src-mediated activation of alpha-diacylglycerol kinase is required for hepatocyte growth factor-induced cell motility. EMBO J. 2000;19:4614-4622.
34. Strasly M, Cavallo F, Geuna M, et al. IL-12 inhibition of endothelial cell functions and angiogenesis depends on lymphocyte-endothelial cell cross-talk. J Immunol. 2001;166:3890-3899.
35. Roca C, Primo L, Valdembri D, et al. Hyperthermia inhibits angiogenesis by a plasminogen activator inhibitor 1-dependent mechanism. Cancer Res. 2003;63:1500-1507.
36. Valdembri D, Serini G, Vacca A, Ribatti D, Bussolino F. In vivo activation of JAK2/STAT-3 pathway during angiogenesis induced by GM-CSF. FASEB J. 2002;16:225-227.
37. Sgadari C, Bacillari G, Toschi E, et al. HIV protease inhibitors are potent anti-angiogenic molecules and promote regression of Kaposi's sarcoma. Nat Med. 2002;8:225-232.
38. Soldi R, Mitola S, Strasly M, Defilippi P, Tarone G, Bussolino F. Role of alphavbeta3 integrin in the activation of vascular endothelial growth factor receptor-2. EMBO J. 1999;18:882-892.
39. Albini A, Soldi R, Giunciuglio D, et al. The angiogenesis induced by HIV-1 tat protein is mediated by the Flk-1/KDR receptor on vascular endothelial cells. Nat Med. 1996;2:1371-1375.
40. Ylikorkala A, Rossi DJ, Korsisaari N, et al. Vascular abnormalities and deregulation of VEGF in

Lkb1-deficient mice. Science. 2001;293:1323-1326.

41. Poole TJ, Finkelstein EB, Cox CM. The role of FGF and VEGF in angioblast induction and migration during vascular development. Dev Dyn. 2001;220:1-17.
42. Serini G, Ambrosi D, Giraudo E, Gamba A, Preziosi L, Bussolino F. Modeling the early stages of vascular network assembly. EMBO J. 2003;22:1771-1779.
43. Thomas KA. Vascular endothelial growth factor, a potent and selective angiogenic agent. J Biol Chem. 1996;271:603-606.
44. Feng G. Shp-2 tyrosine phosphatase: signaling one cell or many. Exp Cell Res. 1999;253:47-54.
45. Tonks NK, Neel BG. Combinatorial control of the specificity of protein tyrosine phosphatases. Curr Opin Cell Biol. 2001;13:182-195.
46. Kroll J, Waltenberger J. The vascular endothelial growth factor receptor KDR activates multiple signal transduction pathways in porcine aortic endothelial cells. J Biol Chem. 1997;272:32521-32527.
47. Scheving LA, Stevenson MC, Taylormoore JM, Traxler P, Russell WE. Integral role of the EGF receptor in HGF-mediated hepatocyte proliferation. Biochem Biophys Res Commun. 2002;290:197-203.
48. Melaragno MG, Fridell YW, Berk BC. The Gas6/Axl system: a novel regulator of vascular cell function. Trends Cardiovasc Med. 1999;9:250-253.
49. Fiebeler A, Park JK, Muller DN, et al. Growth arrest specific protein 6/Axl signaling in human inflammatory renal diseases. Am J Kidney Dis. 2004;43:286-295.
50. Wimmel A, Glitz D, Kraus A, Roeder J, Schuermann M. Axl receptor tyrosine kinase expression in human lung cancer cell lines correlates with cellular adhesion. Eur J Cancer. 2001;37:2264-2274.
51. Sun WS, Misao R, Iwagaki S, Fujimoto J, Tamaya T. Coexpression of growth arrest-specific gene 6 and receptor tyrosine kinases, Axl and Sky, in human uterine endometrium and ovarian endometriosis. Mol Hum Reprod. 2002;8:552-558.
52. Bagowski CP, Stein-Gerlach M, Choidas A, Ullrich A. Cell-type specific phosphorylation of threonines T654 and T669 by PKD defines the signal capacity of the EGF receptor. EMBO J. 1999;18:5567-5576.
53. Miao H, Burnett E, Kinch M, Simon E, Wang B. Activation of EphA2 kinase suppresses integrin function and causes focal-adhesion-kinase dephosphorylation. Nat Cell Biol. 2000;2:62-69.
54. Mothe I, Ballotti R, Tartare S, Kowalski-Chauvel A, Van Obberghen E. Cross talk among tyrosine kinase receptors in PC12 cells: desensitization of mitogenic epidermal growth factor receptors by the neurotrophic factors, nerve growth factor and basic fibroblast growth factor. Mol Biol Cell. 1993;4:737-746.
55. Amselgruber WM, Schafer M, Sinowatz F. Angiogenesis in the bovine corpus luteum: an immunocytochemical and ultrastructural study. Anat Histol Embryol. 1999;28:157-166.
56. Gerhardt H, Betsholtz C. Endothelial-pericyte interactions in angiogenesis. Cell Tissue Res. 2003;314:15-23.
57. Hood JD, Cheresh DA. Role of integrins in cell invasion and migration. Nat Rev Cancer. 2002;2:91-100.
58. Tulis DA, Mnjoyan ZH, Schiesser RL, et al. Adenoviral gene transfer of fortilin attenuates neointima formation through suppression of vascular smooth muscle cell proliferation and migration. Circulation. 2003;107:98-105.
59. Cossette LJ, Hoglinger O, Mou L, Shen SH. Localization and down-regulating role of the protein tyrosine phosphatase PTP2C in membrane ruffles of PDGF-stimulated cells. Exp Cell Res. 1996;223:459-466.
60. Yu CF, Liu ZX, Cantley LG. ERK negatively regulates the epidermal growth factor-mediated interaction of Gab1 and the phosphatidylinositol 3-kinase. J Biol Chem. 2002;277:19382-19388.
61. Marengere LE, Waterhouse P, Duncan GS, Mittrucker HW, Feng GS, Mak TW. Regulation of T cell receptor signaling by tyrosine phosphatase SYP association with CTLA-4. Science. 1996;272:1170-1173.
62. Doan T, Farmer P, Cooney T, Ali MS. Selective down-regulation of angiotensin II receptor type 1A signaling by protein tyrosine phosphatase SHP-2 in vascular smooth muscle cells. Cell Signal. 2004;16:301-311.
63. Hanafusa H, Torii S, Yasunaga T, Matsumoto K, Nishida E. Shp2, an SH2-containing protein-tyrosine phosphatase, positively regulates receptor tyrosine kinase signaling by dephosphorylating and inactivating the inhibitor Sprouty. J Biol Chem. 2004;279:22992-22995.
64. Milarski KL, Saltiel AR. Expression of catalytically inactive Syp phosphatase in 3T3 cells blocks stimulation of mitogen-activated protein kinase by insulin. J Biol Chem. 1994;269:21239-21243.
65. Xiao S, Rose DW, Sasaoka T, et al. Syp (SH-PTP2) is a positive mediator of growth factor-stimulated mitogenic signal transduction. J Biol Chem. 1994;269:21244-21248.
66. Kim H, Baumann H. Dual signaling role of the protein tyrosine phosphatase SHP-2 in regulating expression of acute-phase plasma proteins by interleukin-6 cytokine receptors in hepatic cells. Mol Cell Biol. 1999;19:5326-5338.
67. Yu CL, Jin YJ, Burakoff SJ. Cytosolic tyrosine dephosphorylation of STAT5. Potential role of SHP-2 in STAT5 regulation. J Biol Chem. 2000;275:599-604.
68. Guo DQ, Wu LW, Dunbar JD, et al. Tumor necrosis factor employs a protein-tyrosine phosphatase to inhibit activation of KDR and vascular endothelial cell growth factor-induced endothelial cell proliferation. J Biol Chem. 2000;275:11216-11221.
69. Seo D, Li H, Guedez L, et al. TIMP-2 mediated angiogenesis: an MMP-independent mechanisms. Cell. 2003;114:171-180.
70. Huang L, Sankar S, Lin C, et al. HCPTPA, a protein tyrosine phosphatase that regulates vascular endothelial growth factor receptor-mediated signal transduction and biological activity. J Biol Chem. 1999;274:38183-38188.
71. Saxton TM, Henkemeyer M, Gasca S, et al. Abnormal mesoderm pattering in mouse embryo mutant for the SH2 tyrosine phosphatase Shp-2. EMBO J. 1997;16:2352-2364.
72. Yu DH, Qu CK, Henegariu O, Lu X, Feng GS. Protein-tyrosine phosphatase Shp-2 regulates cell spreading, migration and focal adhesion. J Biol Chem. 1998;273:21125-21131.
73. Manes S, Mira E, Gomez-Mouton C, Zhao ZJ, Lacalle RA, Martinez AC. Concerted activity of tyrosine phosphatase SHP-2 and focal adhesion kinase in regulation of cell motility. Mol Cell Biol. 1999;19:3125-3135.
74. von Wichert G, Haimovich B, Feng G, Sheetz M. Force-dependent integrin-cytoskeleton linkage formation requires downregulation of focal complex dynamics by Shp-2. EMBO J. 2003;22:5023-5035.
75. Carmeliet P. Angiogenesis in health and disease. Nat Med. 2003;9:653-660.
76. Bussolino F, Mantovani A, Persico G. Molecular mechanisms of blood vessel formation. Trends Biochem Sci. 1997;22:251-256.
77. Benjamin LE, Hemo I, Keshet E. A plasticity window for blood vessel remodeling is defined by pericyte coverage of the preformed endothelial network and is regulated by PDGF-B and VEGF. Development. 1998;125:1591-1598.
78. Kalluri R. Basement membranes: structures, assembly and role in tumor angiogenesis. Nat Rev Cancer. 2003;3:422-433.
79. Yang JC, Haworth L, Sherry RM, et al. A randomized trial of bevacizumab, an anti-vascular endothelial growth factor antibody, for metastatic renal cancer. N Engl J Med. 2003;349:427-434.
80. Hurwitz H, Fehrenbacher L, Novotny W, et al. Bevacizumab plus irinotecan, fluorouracil, and leucovorin for metastatic colorectal cancer. N Engl J Med. 2004;350:2335-2342.